Optics & Laser Technology 41 (2009) 654–658

Contents lists available at ScienceDirect

Optics & Laser Technology

journal homepage: www.elsevier.com/locate/optlastec

Ultra-short optical pulse shaping using semiconductor optical amplifier

H. Aghajanpour [a], V. Ahmadi [b,*], M. Razaghi [b]

[a] Department of Electrical Engineering, Science and Research Branch, Islamic Azad University, Tehran, Iran
[b] Department of Electrical Engineering, Tarbiat Modares University, P.O. Box 14115-143, Tehran, Iran

ARTICLE INFO

Article history:
Received 24 December 2007
Received in revised form
7 July 2008
Accepted 13 September 2008
Available online 5 November 2008

Keywords:
Optical pulse compression
Semiconductor optical amplifier
FWM

ABSTRACT

Optical ultra-short pulse compression and amplification using semiconductor optical amplifier (SOA) is presented. Using pump-probe pulse configuration, we present an SOA model which includes the nonlinear effects such as, spectral hole burning (SHB), carrier heating (CH), two-photon absorption (TPA) and group velocity dispersion (GVD) taking into account gain spectrum effect. Then by adjusting time delay between the pump pulse and probe pulse we use the model for simultaneous compression and amplification of probe pulse. We also analyze the four wave mixing (FWM) signal during pulse compression process. It is shown that dispersive effect of GVD on output probe pulse becomes more important for larger cavity length and probe-pump pulses relative time delays.

1. Introduction

In ultra-fast data processing and high-speed optical communication systems, generation and reshaping of ultra-short pulses in semiconductor optical amplifiers (SOA's) becomes of great importance for applications such as optical frequency conversion and optical switches [1]. That is because of some advantages of the SOA which include, compactness and ability to be integrated with other optical devices and, moreover, simultaneous amplification and compression of the optical pulses. Optical pulse compression using pump and probe configuration has already been reported [2]. In this work, we use finite difference-beam propagation method (FD-BPM) [3] to solve the nonlinear Schrödinger equation for linear polarized traveling wave. Using this method, we can consider nonlinear effects such as self-phase modulation (SPM), two-photon absorption (TPA), spectral hole burning (SHB), carrier heating (CH), wavelength dependence of the gain profile and group velocity dispersion (GVD) in the model, which to our knowledge the GVD has not been taken into account in the optical pulse shaping, yet. Effect of GVD cannot be neglected for sub-picosecond pulse durations [4]. In this work, the effect of GVD on output probe pulse characteristics in picosecond regime is obtained numerically, considering the effect of SOA cavity length and the time delay between the probe and pump pulses. Based on the model, we study the nondegenerate four wave mixing signal (FWM) characteristics, and for the first time its dependency on the frequency detuning and time delay between input probe and pump pulses. In Section 2, the equations that describe the propagation of pump and probe pulses are derived. In Section 3, the results are presented and they are discussed. Finally, our work is summarized in Section 4.

2. Theory

Propagation of the optical pulse inside the SOA is defined by the following modified nonlinear Schrödinger equation [5]:

$$\left[\frac{\partial}{\partial z}-\frac{i}{2}\beta_2\frac{\partial^2}{\partial\tau^2}+\frac{\gamma}{2}+\left(\frac{\gamma_{2p}}{2}+ib_2\right)|V(\tau,z)|^2\right]V(\tau,z)$$
$$=\left\{\frac{1}{2}g_N(\tau)\left[\frac{1}{f(\tau)}+i\alpha_N\right]+\frac{1}{2}\Delta g_T(\tau)(1+i\alpha_T)\right.$$
$$\left.-\frac{i}{2}\frac{\partial g(\tau,\omega)}{\partial\omega}\bigg|_{\omega_0}\frac{\partial}{\partial\tau}-\frac{1}{4}\frac{\partial^2 g(\tau,\omega)}{\partial\omega^2}\bigg|_{\omega_0}\frac{\partial^2}{\partial\tau^2}\right\}V(\tau,z) \quad (1)$$

here

$$g_N(\tau)=g_0\exp\left(-\frac{1}{W_s}\int_{-\infty}^{\tau}e^{-s/\tau_s}|V(s)|^2\,ds\right) \quad (2)$$

$$f(\tau)=1+\frac{1}{\tau_i P_i}\int_{-\infty}^{\infty}u(s)e^{-s/\tau_i}|V(\tau-s)|^2\,ds \quad (3)$$

$$\Delta g_T(\tau)=-h_1\int_{-\infty}^{\infty}u(s)e^{-s/\tau_{ch}}(1-e^{-s/\tau_i})|V(\tau-s)|^2\,ds$$
$$-h_2\int_{-\infty}^{\infty}u(s)e^{-s/\tau_{ch}}(1-e^{-s/\tau_i})|V(\tau-s)|^4\,ds \quad (4)$$

* Corresponding author. Tel./fax: +98 21 82883368.
E-mail address: v_ahmadi@modares.ac.ir (V. Ahmadi).

0030-3992/$ - see front matter © 2008 Elsevier Ltd. All rights reserved.
doi:10.1016/j.optlastec.2008.09.007

$$\frac{\partial g(\tau,\omega)}{\partial \omega}|\omega_o = A_1 + B_1[g_0 - g(\tau,\omega_o)] \quad (5)$$

$$\frac{\partial^2 g(\tau,\omega)}{\partial \omega^2}|\omega_0 = A_2 + B_2[g_0 - g(\tau,\omega_0)] \quad (6)$$

$$g(\tau,\omega_0) = g_N(\tau,\omega_0)/f(\tau) + \Delta g_T(\tau,\omega_0) \quad (7)$$

where $V(\tau, z)$ is slowly varying envelope function of an optical pulse, $\tau = t - z/v_g$, v_g is group velocity, γ is linear loss, γ_{2p} is the TPA coefficient, β_2 is the GVD, $b_2 = \omega_0 n_2/cA$, n_2 is the nonlinear refractive index, ω_0 is the central angular frequency, c is the velocity of light in vacuum and A is the effective area, respectively. $g_N(\tau)$ is saturated gain due to carrier depletion, g_0 is the linear gain, W_s is the saturation energy, τ_s is the carrier lifetime, $f(\tau)$ is the spectral-hole burning function, P_i is the SHB saturation power, τ_i is the intraband relaxation time, α_N and α_T are the linewidth enhancement factors associated with gain changes due to carrier depletion and CH, respectively. $\Delta g_T(\tau)$ is the resulting gain changes due to CH and TPA, $u(s)$ is the unit step function, τ_{ch} is the CH relaxation time, h_1 is the contribution of stimulated emission and free-carrier absorption to CH gain reduction, and h_2 is contribution of TPA. Finally, A_1 and A_2 are the slope and the curvature of linear gain at central frequency, respectively, and B_1 and B_2 are constants describing changes in these quantities with saturation. We use the parameters of the GaAs/AlGaAs SOA with wavelength of 0.86 μm and length of 500 μm. The two input optical pulses (pump and probe pulse) that are injected from the same facet (co-propagation configuration) are expressed by

$$V(\tau) = V_p(\tau) + V_q(\tau)\exp(-i\Delta\omega\tau) \quad (8)$$

Here $V_p(\tau)$ and $V_q(\tau)$ are the complex envelope functions of the input pump and probe pulses, respectively, and $\Delta\omega = 2\pi(f_p - f_q)$ where f_p and f_q are the central frequencies of the input pump pulse and probe pulse, respectively. It is assumed that input probe pulse intensity is sufficiently small (20 times smaller than of pump pulse energy), so that it does not modify the optical properties of the SOA. Input pulse shape is Gaussian and is Fourier transform limited. The effect of input pulse duration becomes of most importance when we use the device in saturation regime. The longer durations result in the higher output saturation energies because of the fast response of the spectral-hole burning and CH [6]. We have solved the equation using FD-BPM, to analyze all the nonlinear parameters, numerically.

3. Results and discussion

3.1. Compression and amplification

Fig. 1 shows the normalized input and output probe pulse shapes when both of the pump and probe pulses are injected into the SOA at the same time (time delay equals to zero). Here, pump pulse and probe pulse energies are 20 and 1 pJ, respectively, frequency detuning is 1 THz and the duration of input probe pulse and input pump pulse are 12 and 2 ps, respectively. In this condition the leading edge of probe pulse experiences unchanged gain and is linearly amplified. But for the trailing edge this is not the case. Pump pulse saturates the gain medium by carrier consumption and the trailing edge of probe pulse sharply damps. The dynamic gain response of the SOA to the pump pulse is presented in Fig. 2. All the parameters used here are the same as those in Fig. 1. The step-like profile in Fig. 2, results from carrier depletion induced by pump pulse. Quick gain depletion occurs near the zero time, when the peak power of the pump pulse appears, due to the effects of fast processes such as CH and SHB [7,8]. The magnitude of recovering gain is proportionally

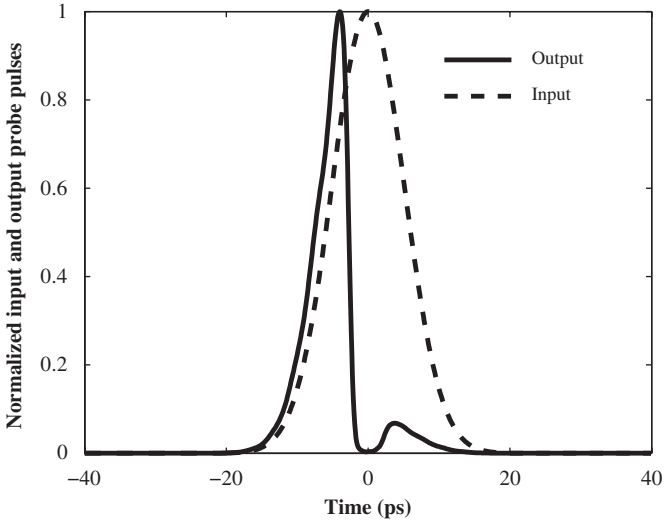

Fig. 1. Normalized input and output probe pulse shapes. Pump pulse energy is 20 pJ and frequency detuning is 1 THz. The pump and probe pulse widths are 2 and 12 ps, respectively.

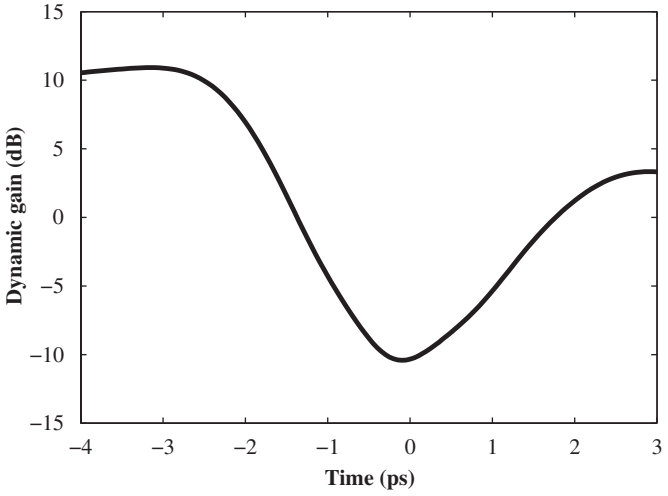

Fig. 2. Gain dynamic response of the SOA to the pump pulse corresponding to Fig. 1.

dependent upon pump pulse energy. It can be explained by carrier generation through the absorption of energy from the pump pulse because of the TPA [9]. Utilizing this dynamic gain, we can explain the output probe pulse shape at different time delays. Fig. 3 shows the output probe pulse width as a function of time delay between the probe pulse and pump pulse for two different energy values of pump pulses, 20 and 50 pJ. Here, negative time delay means probe pulse is ahead of pump pulse and positive time delay means probe pulse lags behind pump pulse.

In negative time delays, where the whole probe pulse is ahead of pump pulse, the full pulse experiences a constant gain due to its low energy. Thus, probe pulse is amplified linearly and pulse shape remains unchanged. By changing time delay between the pump pulse and probe pulse, there is overlap between trailing edge of probe pulse and leading edge of pump pulse. So, this part of probe pulse will see the decreased gain while the other part is amplified with the unsaturated gain. Therefore, signal pulse-width compression starts. With increasing the overlap, signal pulse width is further decreased with a two-peak structure. In

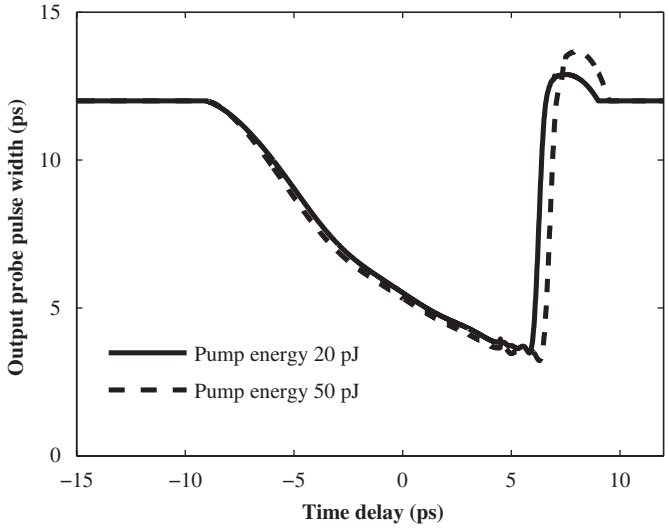

Fig. 3. Output probe pulse width as a function of time delay between the pump pulse and the probe pulse. The parameters are the same as those in Fig. 1.

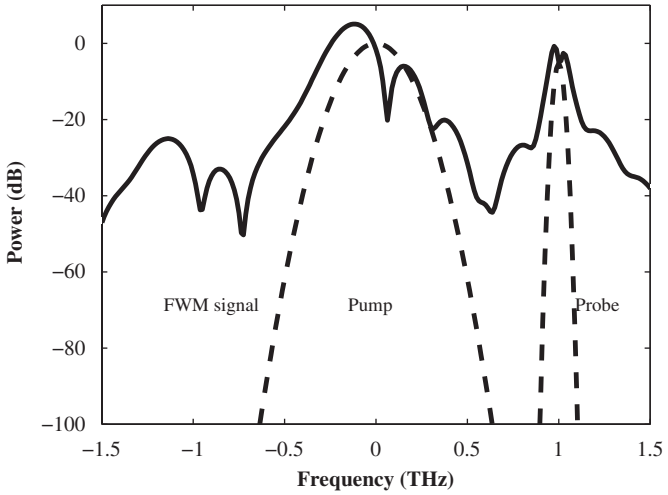

Fig. 5. Frequency spectra of the input (dashed line) and output (solid line) pulse. Pump pulse energy is 20 pJ and frequency detuning is 1 THz. Other parameters are the same as those in Fig. 1.

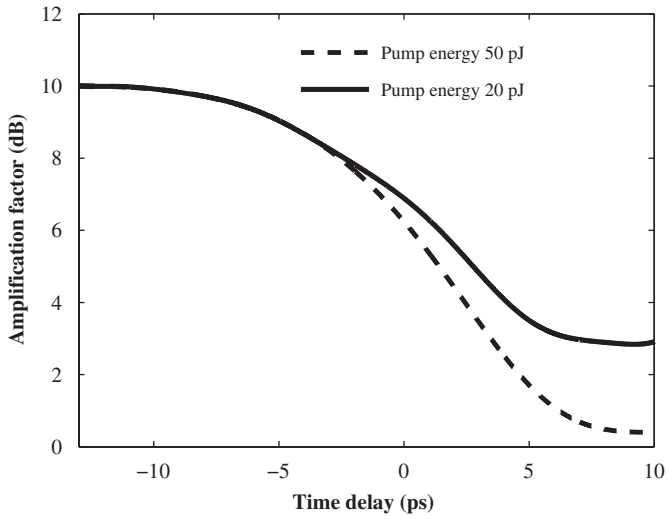

Fig. 4. Amplification factor of the probe pulse as a function of time delay between the input pulses, corresponding to Fig. 3.

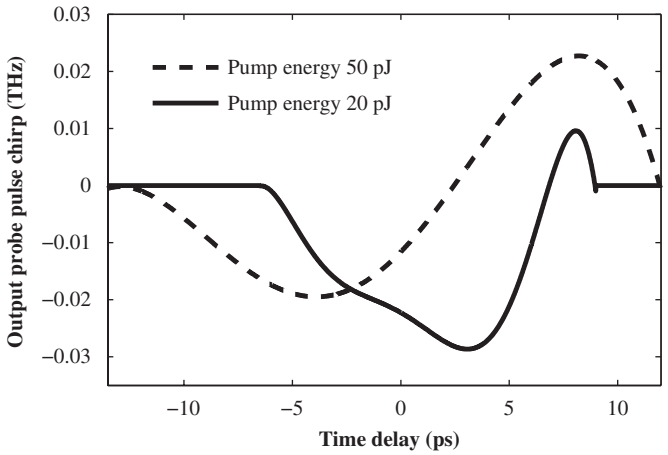

Fig. 6. Output probe pulse chirp for two different input pump pulse energies.

positive time delay region, when both of the two peaks are more than 0.5, pulse width is broadened. The maximum amount of probe pulse compression using this structure is ~4.

Another important parameter is the amplification factor, which is defined as the ratio of output probe pulse energy to the input probe pulse energy. Fig. 4 illustrates the amplification factor corresponding to Fig. 3. We can see here the effect of gain saturation on probe pulse amplification. The saturation effect is increased for large positive time delays and higher pump energies.

3.2. Frequency domain

Fig. 5 shows the input and output signal spectrum corresponding to Fig. 1. In the output spectrum there is a new signal which has a peak position at −1 THz. When there is a frequency detuning between input pulses in SOA this signal is generated by FWM process. Also, one can see higher order of frequency mixings in the output spectrum, by widening the sampled frequency range. The high values of energy of the pump pulse results in a frequency shift in peak power of output signal pulses. Fig. 6 illustrates the output probe pulse chirp versus time delay between the two input pulses for two different values of pump energy, 20 and 50 pJ. By varying time delay, the overlap between two pulses varies and output spectrum changes. Higher pump energy (50 pJ) gives a symmetrical chirp versus time delay in two regions. The positive chirp peak occurs at ~8 ps and its value is higher for larger pump energy. The negative chirp peak moves from 3.5 ps towards −4.7 ps whose value is inversely proportional to pump pulse energy. The peak values of pulse chirp are determined by ultrafast dynamic process and carrier depletion induced by pump pulse [10,11].

As mentioned above, in the output pulse spectrum there is a third pulse, FWM signal, whose energy is obviously small compared to the other output pulses. In Fig. 7, we can see the variation of the FWM signal energy versus time delay between input pump pulse and probe pulse, for two different pump pulse energies. The other parameters are the same as those in Fig. 6. In the vicinity of zero time delay the FWM signal energy reaches its peak value, ~0.12 pJ. By inserting time delay between input pulses, this value decreases. This means that, the FWM energy is

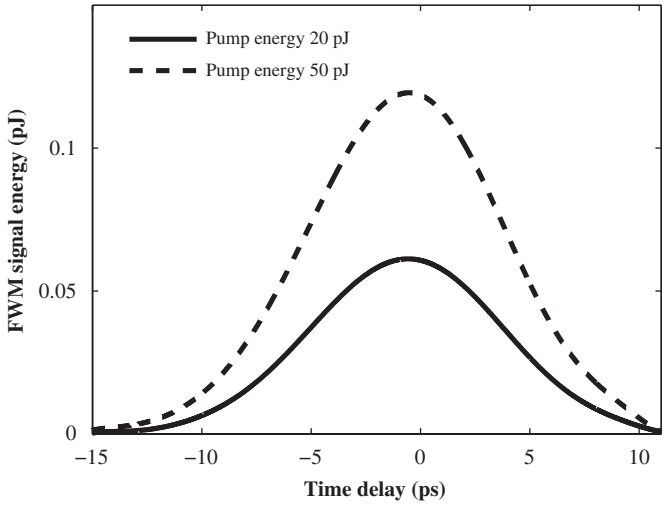

Fig. 7. FWM signal energy as a function of time delay between two input pulses, pump energy is 20 (solid line) and 50 pJ (dashed line), respectively.

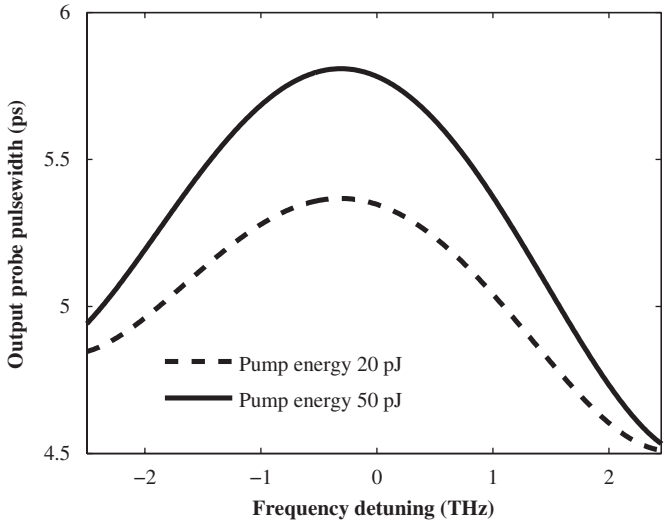

Fig. 8. Output probe pulse width as a function of frequency detuning between input pulses. The parameters are the same as those in Fig. 7.

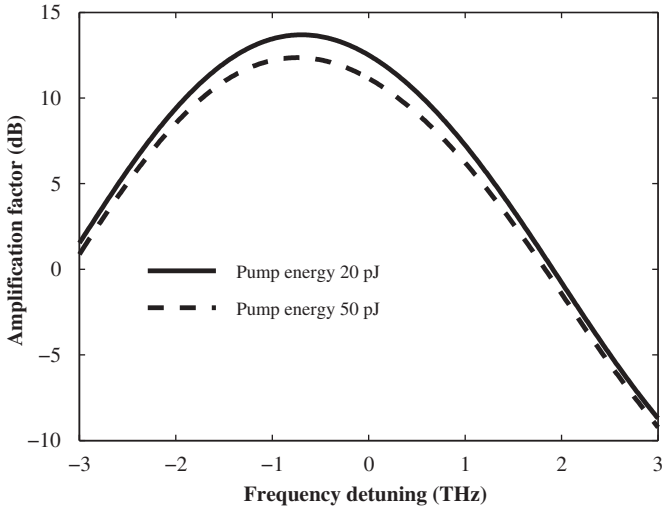

Fig. 9. Amplification factor of probe pulse versus frequency detuning. The parameters are the same as those in Fig. 7.

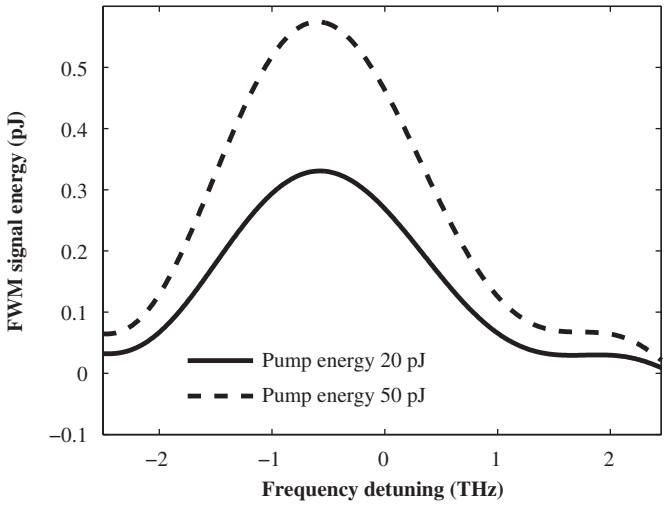

Fig. 10. FWM signal energy versus frequency detuning. The parameters are the same as those in Fig. 7.

proportional to product of the intensities of the overlap between the pump pulse and probe pulse.

A very important parameter in the pump-probe pulse amplification in SOA is frequency detuning between two input pulses. Pump pulse central frequency is tuned at the gain peak and probe pulse is injected by frequency detuning with respect to pump pulse. Fig. 8 illustrates the output probe pulse width versus the frequency detuning. It shows that, by increasing the frequency detuning, the probe pulse width is further decreased. But in Fig. 9, which shows the amplification factor versus frequency detuning, larger detuning results in a smaller amplification factor. Therefore, there is a trade off between two important parameter, compression factor and amplification factor of probe pulse. In this work, frequency detuning is 1 THz that results in a compression factor of about 4 and amplification factor of 6.5 and 5.5 dB for 20 and 50 pJ pump pulse energies, respectively.

Meanwhile, in Fig. 8, for both 20 and 50 pJ pump pulse, the peak value of output pulse width occurs at $\simeq$0.7 THz. This can be explained by Fig. 9. As a result of gain saturation due to strong pump pulse, the peak value moves toward lower frequency side.

Finally, the FWM signal energy versus frequency detuning for different pump pulse energies, 20 and 50 pJ, is shown in Fig. 10. It shows that, the FWM signal energy increases with pump pulse energy and decreases with frequency detuning.

3.3. Group velocity dispersion

To see the effect of GVD on output probe characteristics we apply very short pulses in the range of picosecond. Fig. 11 shows the output probe peak shift versus time delay between input pulses for different values of GVD. Input pump and probe pulsewidths are 1 and 8 ps, respectively. Pump pulse energy is 20 pJ which is 20 times greater than that of probe pulse and frequency detuning is 2 THz. The amount of peak shift is larger for greater values of GVD. The GVD effect increases from positive time delays towards negative time delays. For positive time delays the pump pulse is ahead of probe pulse and saturation effect of strong pump pulse is dominant. By changing time delay toward negative

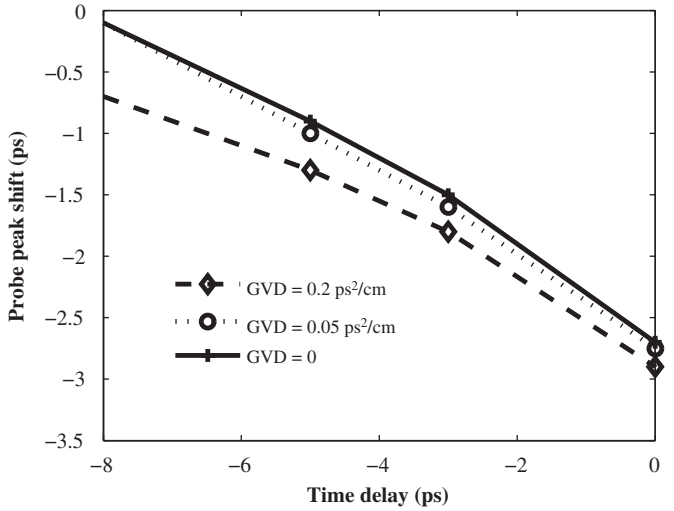

Fig. 11. Probe peak shift versus time delay between the input pump and probe pulse for different GVD values. Pump and probe are 1 and 8 ps, respectively. Pump energy is 20 pJ and 20 times greater than that of probe. Frequency detuning is 2 THz.

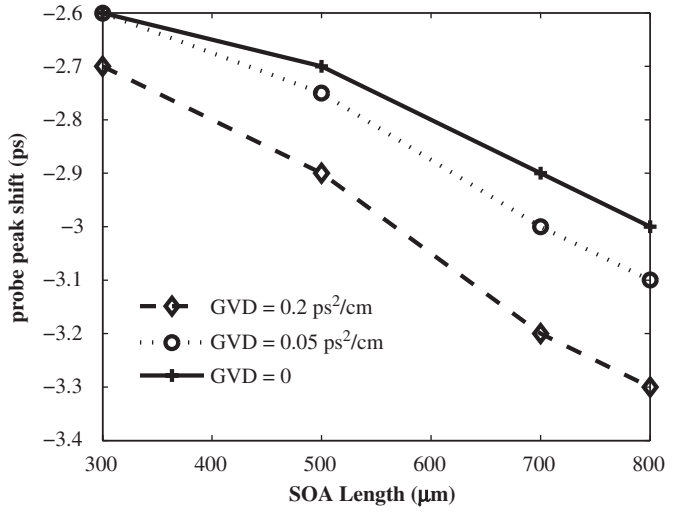

Fig. 12. Probe peak shift versus SOA length. The parameters are the same as those in Fig. 11.

region the overlap between pulses decreases. For more negative time delays pump is behind the probe pulse and effect of increase in GVD leads to further movement in probe peak position.

Fig. 12 illustrates the probe peak shift versus the length of the amplifier when there is no time delay between input pulses. GVD effect on probe peak shift is greater in the longer cavity SOA. To our knowledge, the dispersive effects of GVD on probe pulse shape shown in Figs. 11 and 12 have not been considered so far.

4. Conclusion

In this work, we have numerically analyzed the optical pump-probe pulse characteristics in the SOA by the FD-BPM. It is shown that using an input strong pump pulse and by adjusting the time delay between two pulses, one can control both amplification and compression of probe pulse. Output signal spectrum, FWM signal characteristics and output probe pulse chirp numerically have been studied. We have shown that, a probe pulse compression factor of about 4 can be obtained by this approach. We have studied the dispersive effect of GVD on output pulse shape, which has not been considered yet. It was shown that there is a larger probe peak shift for larger SOA cavity length and probe-pump pulses relative time delay. This method can be used for high-efficiency wavelength converters and optical switching systems.

Acknowledgement

This work was partially supported by the Iran Telecommunication Research Centre (ITRC).

References

[1] Downey PM, Bowers JE, Tucker RS, Agyekum E. Picosecond dynamics of a gain-switched InGaAsP laser. IEEE J Quantum Electron QE 1987;23:1039–47.
[2] Tang JM, Shore KA. Active picosecond optical pulse compression in semiconductor optical amplifiers. IEEE J Quantum Electron 1999;35:93–100.
[3] Das NK, Yamayoshi Y, Kawaguchi H. Analysis of basic four-wave mixing characteristics in a semiconductor optical amplifier by the finite-difference beam propagation method. IEEE J Quantum Electron 2000;36:1184–92.
[4] Agrawal GP. Effect of gain dispersion on ultrashort pulse amplification in semiconductor laser amplifiers. IEEE J Quantum Electron 1991;27:1483–848.
[5] Hong MY, Chang YH, Dienes A, Heritage JP, Delfyett PJ, Patterson FG. Femtosecond self- and cross-phase modulation in semiconductor laser amplifier. IEEE J Select Topics Quantum Electron 1996;2:523–39.
[6] Hall KL, Lenz G, Darwish AM, Ippen EP. Subpicosecond gain and index dynamics in InGaAsP diode lasers. Opt Commun 1994;111:589–612.
[7] Tang JM, Spenser PS, Shore KA. Effect of semiconductor nonlinear gain on the chirp and spectral properties of amplified subpicosecond optical pulses. Electron Lett 1996;32:1293–4.
[8] Saleh AAM, Jopson RM, Darcie TE. Compensation of nonlinearity in semiconductor optical amplifiers. Electron Lett 1998;24:950–2.
[9] Tang JM, Shore KA. Strong picosecond optical pulse propagation in semiconductor optical amplifiers at transparency. IEEE J Quantum Electron 1998;34:1263–9.
[10] Mecozzi A, Mork J. Saturation induced by picosecond pulses in semiconductor optical amplifiers. J Opt Soc Am B 1997;14:761–70.
[11] Tang JM, Spenser PS, Shore KA. The influence of gain compression on picosecond optical pulses in semiconductor optical amplifiers. J Mod Opt 1998;45:1211–8.